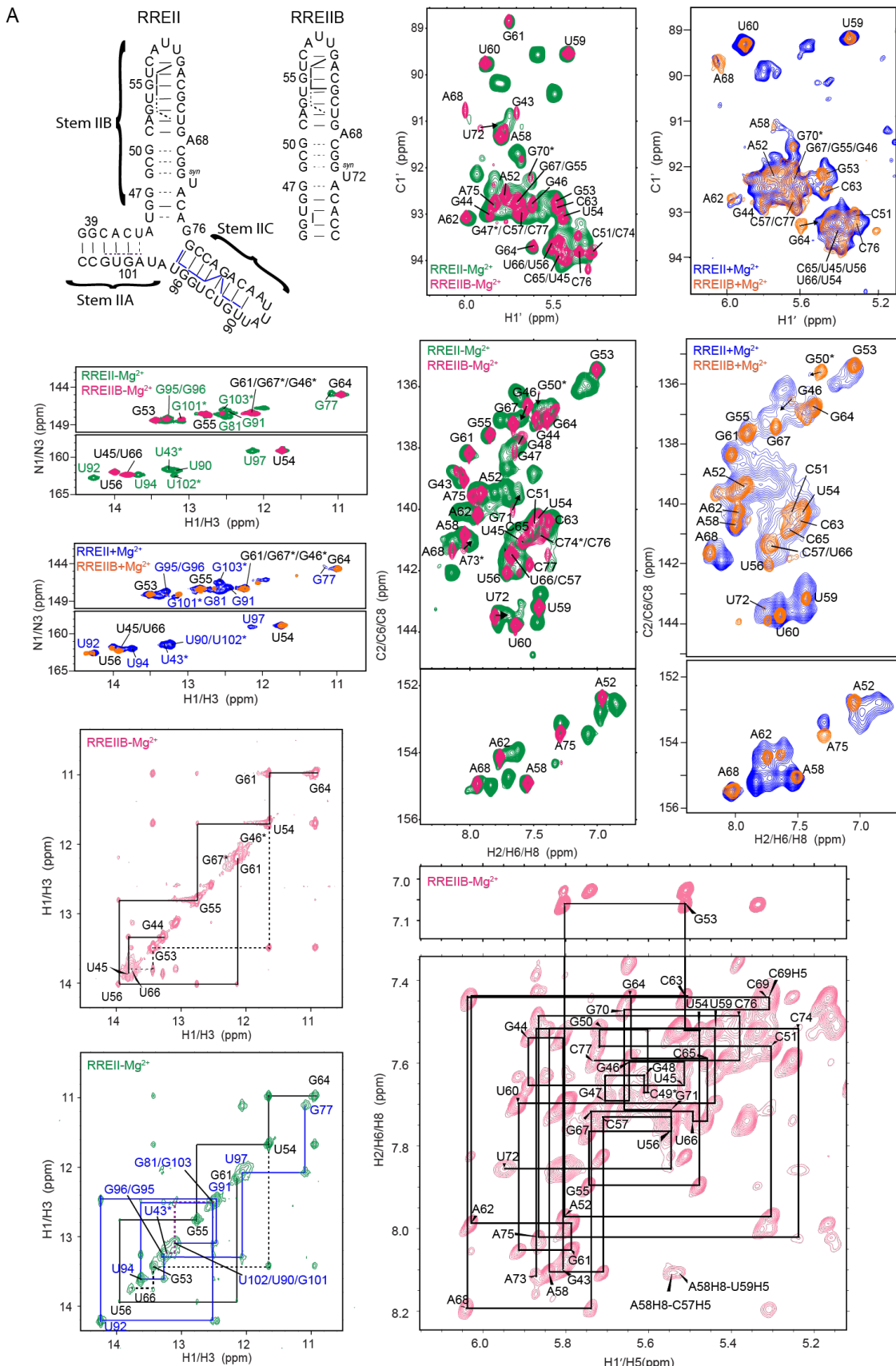
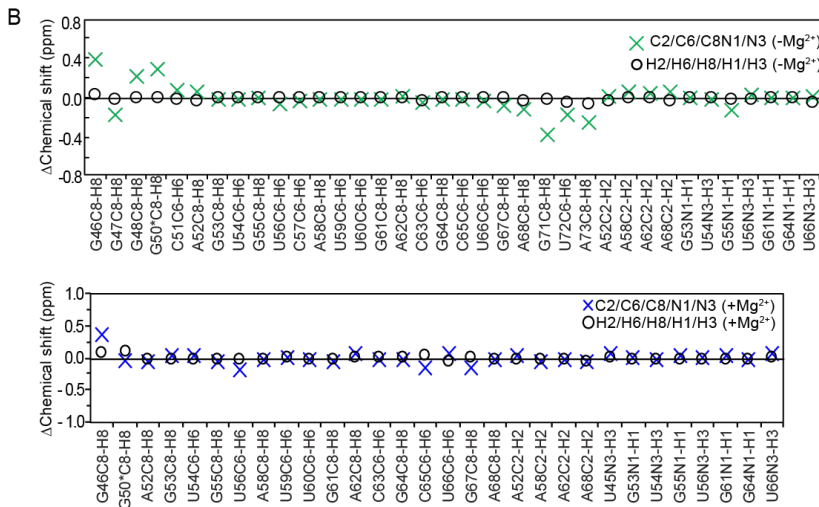


**Dynamic ensemble of HIV-1 RRE stem IIB reveals non-native conformations that disrupt the Rev binding site**

Chia-Chieh Chu<sup>1</sup>, Raphael Planger<sup>2</sup>, Christoph Kreutz<sup>2</sup>, and Hashim M. Al-Hashimi\*<sup>1,3</sup>

**Supplementary data**





**Figure S1.** NMR spectra measured for RREIIB and RREII. (A) 2D  $^1\text{H}$ - $^1\text{H}$  NOESY spectra of exchangeable (10 °C in 10%  $\text{D}_2\text{O}$  and mixing time 180 ms) and nonexchangeable (37 °C in 100%  $\text{D}_2\text{O}$  and mixing time 220 ms) protons showing distance based connectivity highlighted on the secondary structure. Base pairs with and without detectable H-bonding are indicated using solid and dashed lines, respectively. Also shown are overlays of 2D  $^1\text{H}$ ,  $^{15}\text{N}$ - and  $^1\text{H}$ ,  $^{13}\text{C}$ -HSQC spectra for RREIIB and RREII recorded at 25 (-Mg<sup>2+</sup>) and 10 °C (+Mg<sup>2+</sup>) respectively. The imino assignments of the residues in RREIIB are black, while green (-Mg<sup>2+</sup>) and blue (+Mg<sup>2+</sup>) in RREII. Resonances with potentially ambiguous resonance assignment are labeled with an asterisk. (B) Differences between RREIIB and RREII chemical shifts measured in the absence and presence of Mg<sup>2+</sup>. Nucleotides with resonances showing large perturbations are highlighted using red circles on the secondary structure. The sample conditions were 1.0-1.2 mM RREII or RREIIB in 15 mM sodium phosphate, 25 mM NaCl, 0.1 mM EDTA, pH 6.4 with or without 3 mM MgCl<sub>2</sub>.

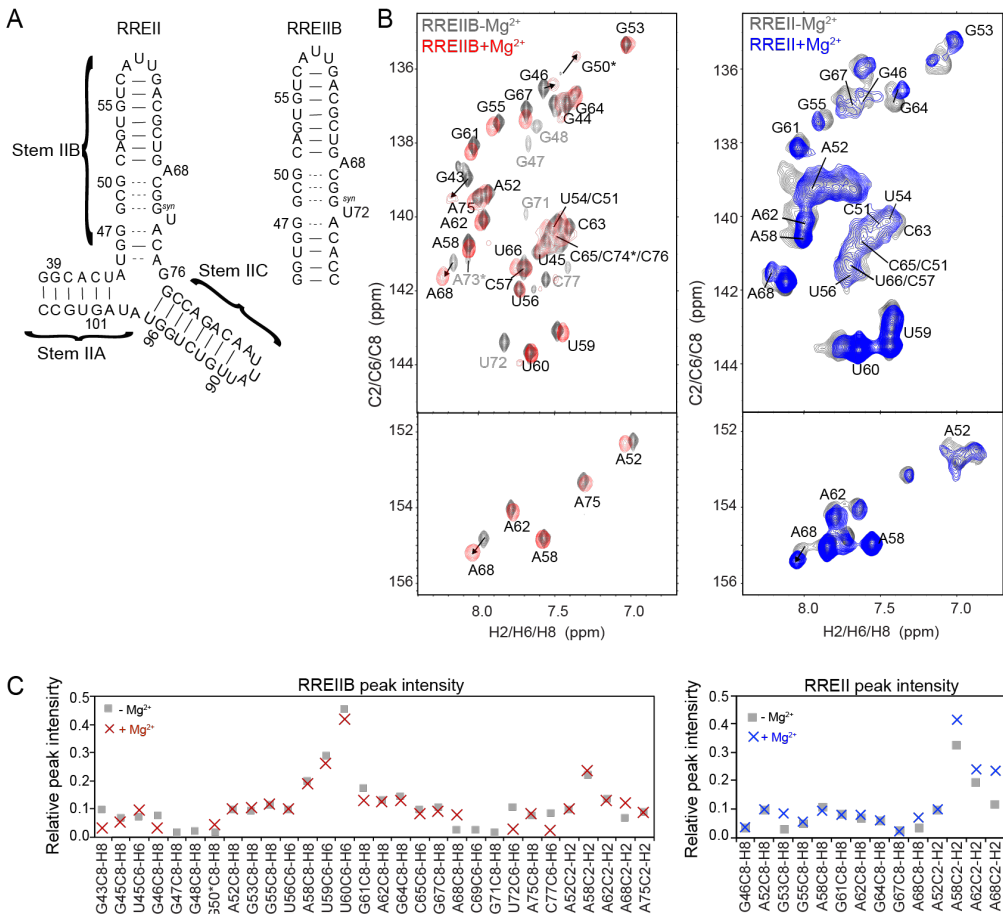


**Figure S2.** Impact of Mg<sup>2+</sup> on spectra of RREIIB and RREII. (A) Secondary structure of RREIIB and RREII. (B) Comparison of 2D <sup>1</sup>H, <sup>13</sup>C-HSQC spectra measured for RREIIB (25 °C) and RREII (10 °C). (C) Normalized resonance intensities measured for RREIIB (at 25 °C) and RREII (at 10 °C) in the presence and absence of 3 mM Mg<sup>2+</sup>. A52-C8H8, A52-C2H2 and U56-C6H6 were used as a reference and normalized to 0.1. The sample conditions were 1.0-1.2 mM RREII or RREIIB in 15 mM sodium phosphate, 25 mM NaCl, 0.1 mM EDTA, pH 6.4 with or without 3 mM MgCl<sub>2</sub>.

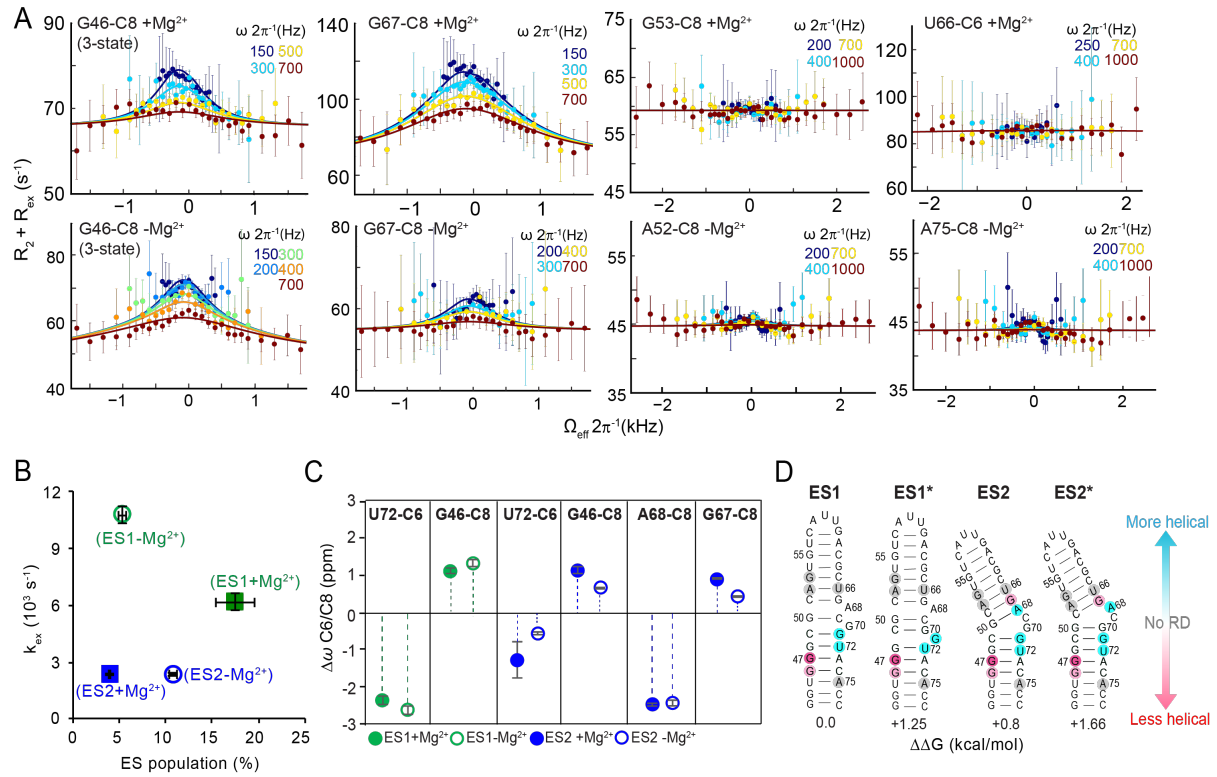


**Figure S3.** RD profiles and exchange parameters measured at 25 °C. (A) RD profiles measured for RREIIB in the absence and presence of  $Mg^{2+}$ . (B) ES population and exchange rate measured for RREIIB ES1 and ES2 in the presence (filled) and absence (open) of  $Mg^{2+}$ . (C) As in main Fig. 3B showing  $\Delta\omega_{\text{RD}}$  in the absence and presence of  $Mg^{2+}$ . (D) Chemical shift fingerprints annotated on the putative structural models for ES1 and ES2 obtained as the top two (following the GS) structures predicted by MC-fold (1). The residues on RREIIB with RD measurements are indicated in circles. Gray: no dispersion, cyan:  $\Delta\omega < 0$ , red:  $\Delta\omega > 0$ . The sample conditions were 1.0–1.2 mM RREIIB in 15 mM sodium phosphate, 25 mM NaCl, 0.1 mM EDTA, pH 6.4 with or without 3 mM  $MgCl_2$ .

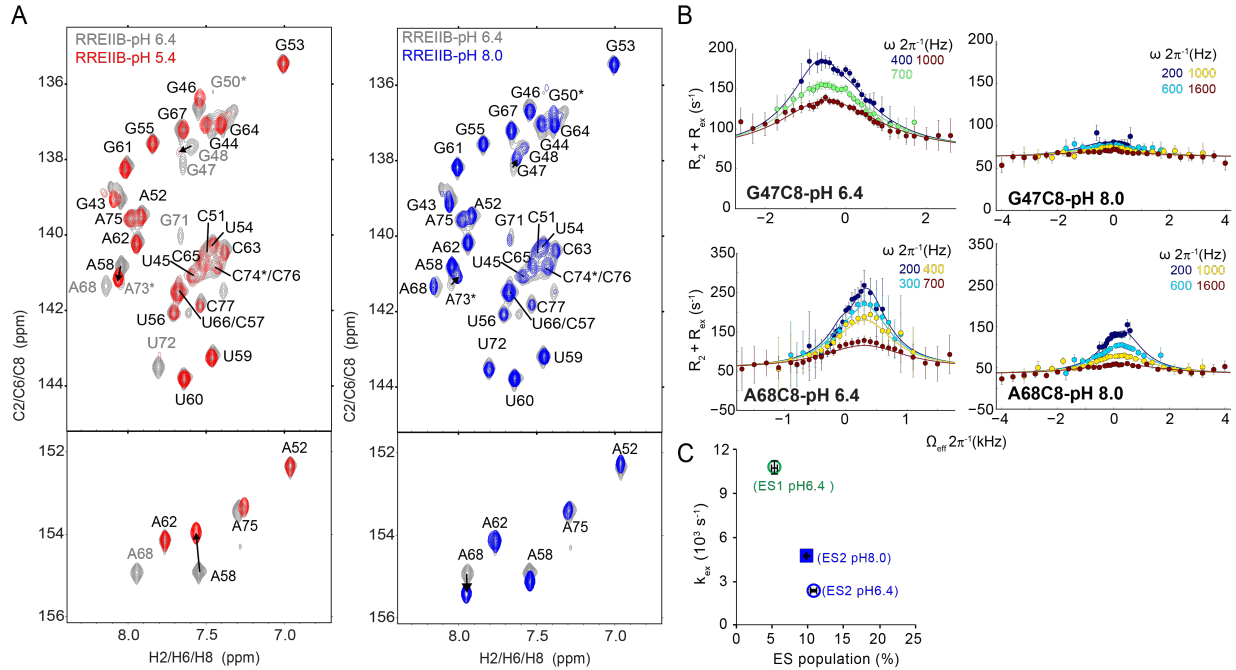


**Figure S4.** pH dependence of  $R_{1\rho}$  RD profiles at 25 °C. (A) Comparison of 2D  $^1\text{H}, ^{13}\text{C}$ -HSQC spectra measured for RREIIB at pH 5.4, 6.4 and 8.0. The resonances with broadening are colored in gray. (B)  $R_{1\rho}$  RD profiles acquired with different color-coded power levels. Solid lines represent the global fits to the RD data (G47-C8 and A68-C8 at pH 6.4 and pH 8.0). Error bars represent experimental uncertainty based on Monte Carlo analysis of monoexponential decay curves and the signal noise. (C) Exchange parameters for ES1 and ES2 from 3-state fit of  $R_{1\rho}$  RD profiles for G47-C8 at pH 6.4 or 8.0. Note that ES1 is undetectable at high pH and  $p_B$  is estimated to be <0.01%. The sample conditions were 1.0–1.2 mM RREIIB in 15 mM sodium phosphate, 25 mM NaCl, 0.1 mM EDTA.

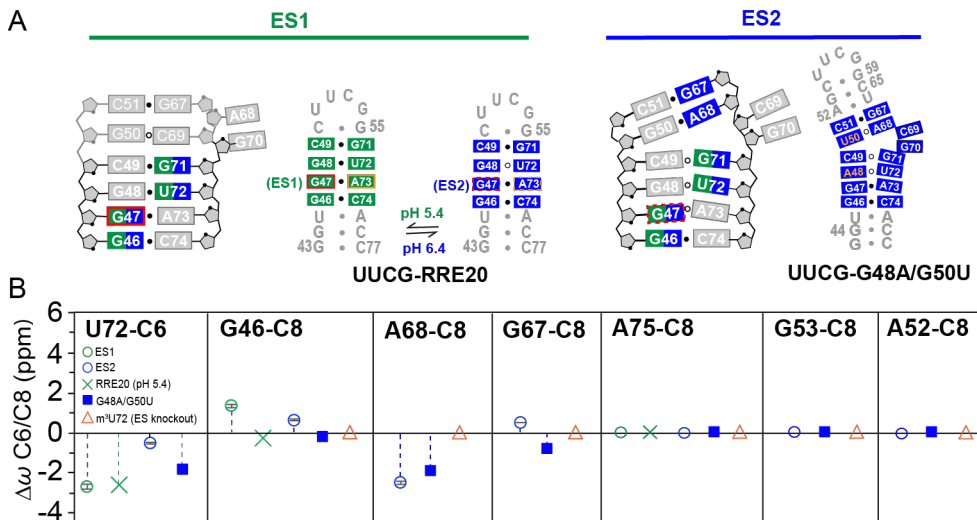


**Figure S5.** Chemical shift fingerprinting of RRE ESs. (A) The designed ES trap mutants for chemical shift fingerprints. *Syn* bases and protonated adenosine are indicated with red and orange boxes, respectively. The G47(*syn*)-A73<sup>+</sup>(anti) ⇌ G47(anti)-A73(anti) equilibrium indicated with dashed red boxes. (B) Comparison of  $\Delta\omega$  obtained for the mutants and using RD in the absence of Mg<sup>2+</sup>. The sample conditions were 1.0-1.2 mM RREIIB in 15 mM sodium phosphate, 25 mM NaCl, 0.1 mM EDTA, pH 6.4.

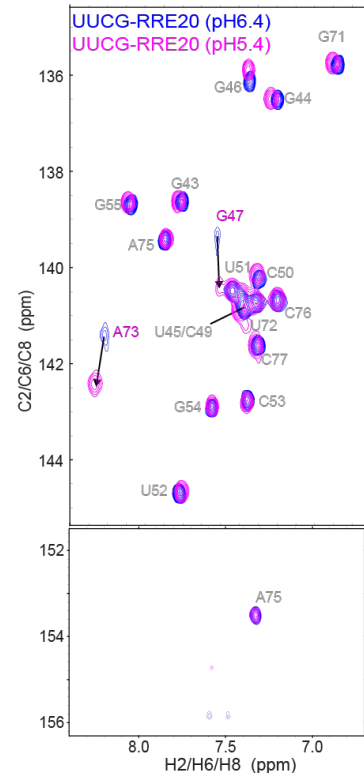
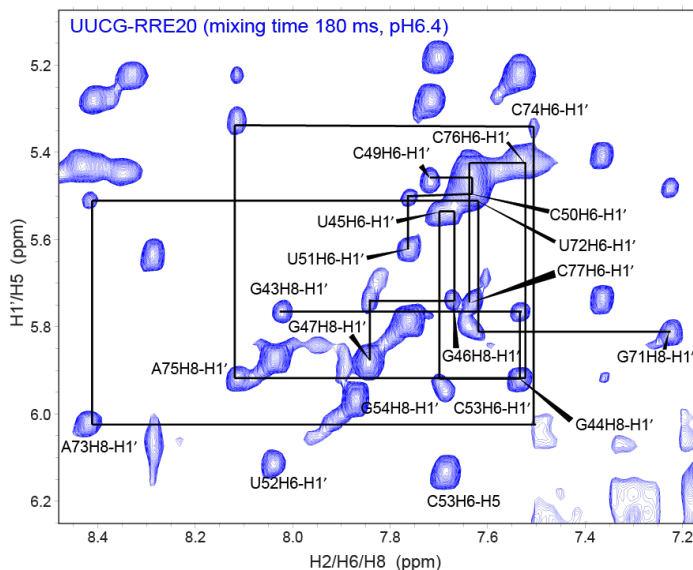
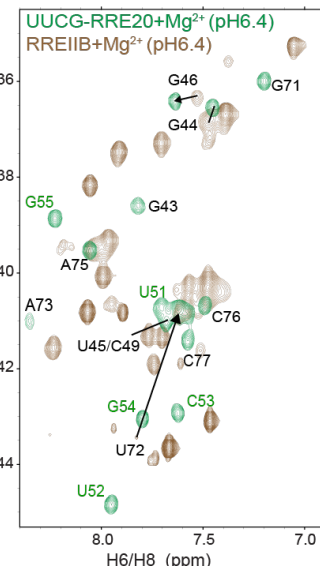
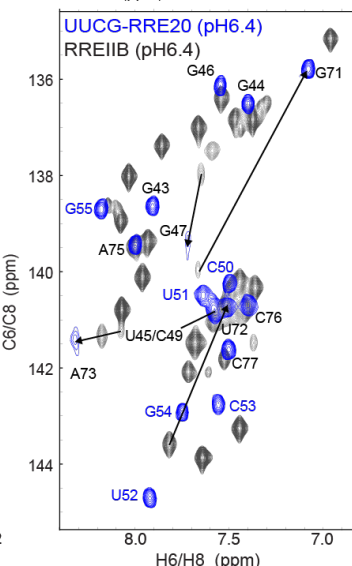
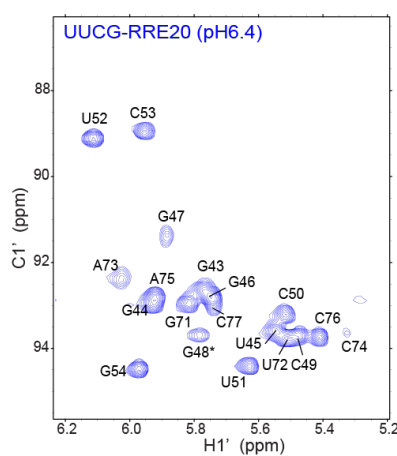
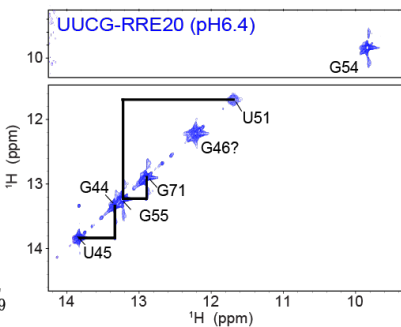
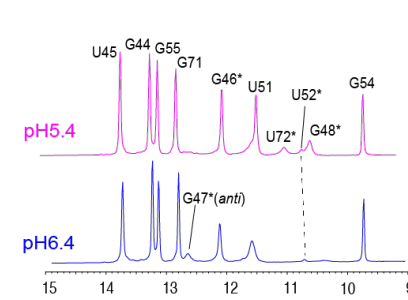
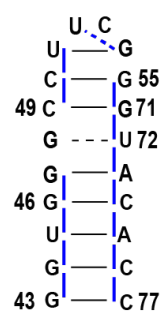
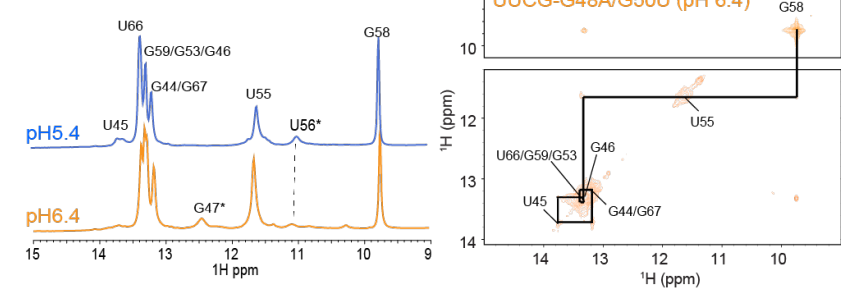
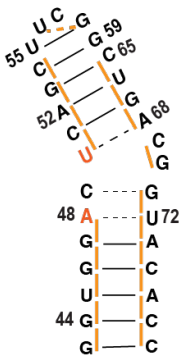
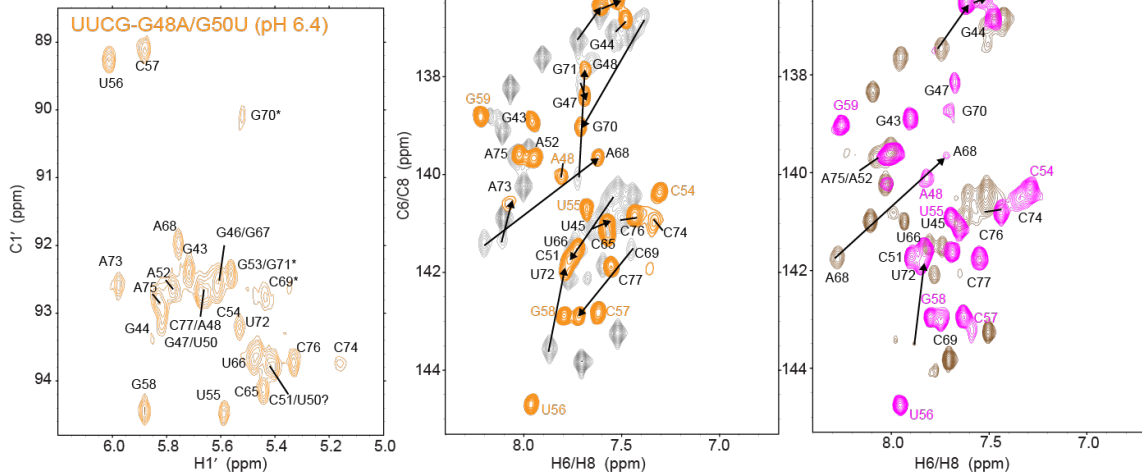


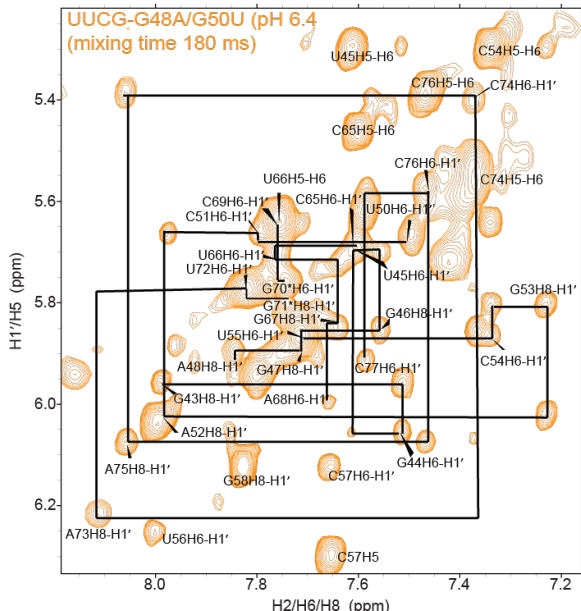
**Figure S6.** NMR spectra and assignments for ES1 stabilizing mutant UUCG-RRE20. Secondary structure of UUCG-RRE20 based on NMR data at 25 °C. At pH 6.4, a weak G47-H1 imino resonance is observed consistent with an *anti* conformation that exchanges with a *syn* conformation (in which imino is not detectable due to solvent exchange). This resonance was broadened out of detection at pH 5.4 consistent with stabilization of a dominant G47(*syn*) conformation. The imino resonances for the adjacent G48-U72 wobble were not observed at pH 6.4, likely due to conformational exchange in the adjacent G-A mismatch, but were observable at pH 5.4 in which the exchange at the adjacent G-A mismatch is reduced. Uninterrupted intra- and inter-nucleotide H8/6-H1' NOEs were observed for all other resonances except G48 (which is broadened out of detection due to exchange) indicating that these nucleotides adopt a helical conformation. Resonances with potentially ambiguous resonance assignment are labeled with an asterisk. The sample condition was 2.0 mM UUCG-RRE20 in 15 mM sodium phosphate, 25 mM NaCl, 0.1 mM EDTA, with or without 3 mM MgCl<sub>2</sub>.



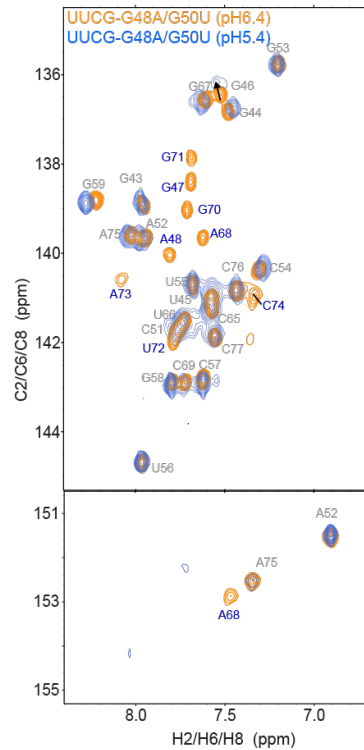
UUCG-G48A/G50U  
(ES2 trap)



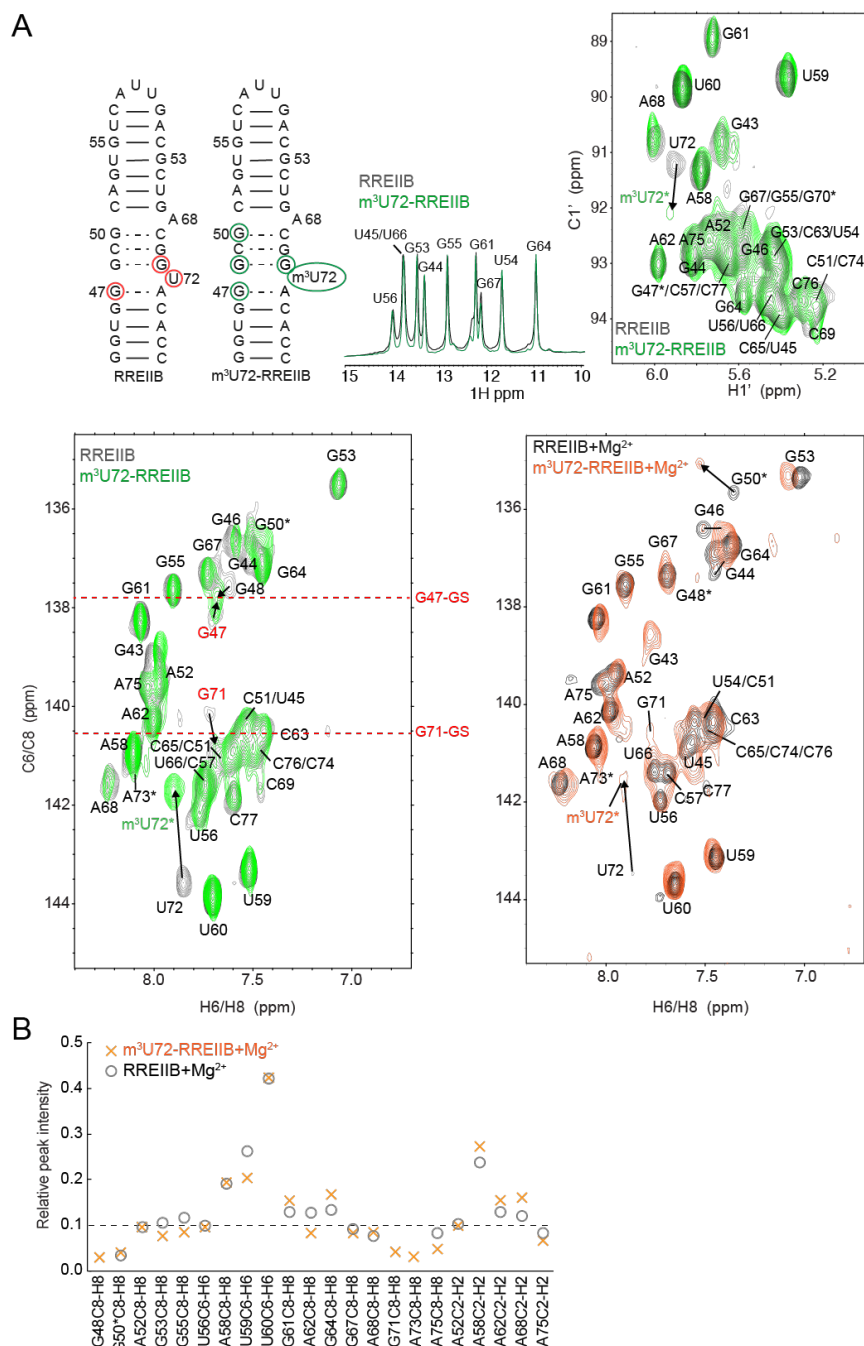
UUCG-G48A/G50U (pH 6.4)  
(mixing time 180 ms) 



UUCG-G48A/G50U (pH6.4)  
UUCG-G48A/G50U (pH5.4) G53

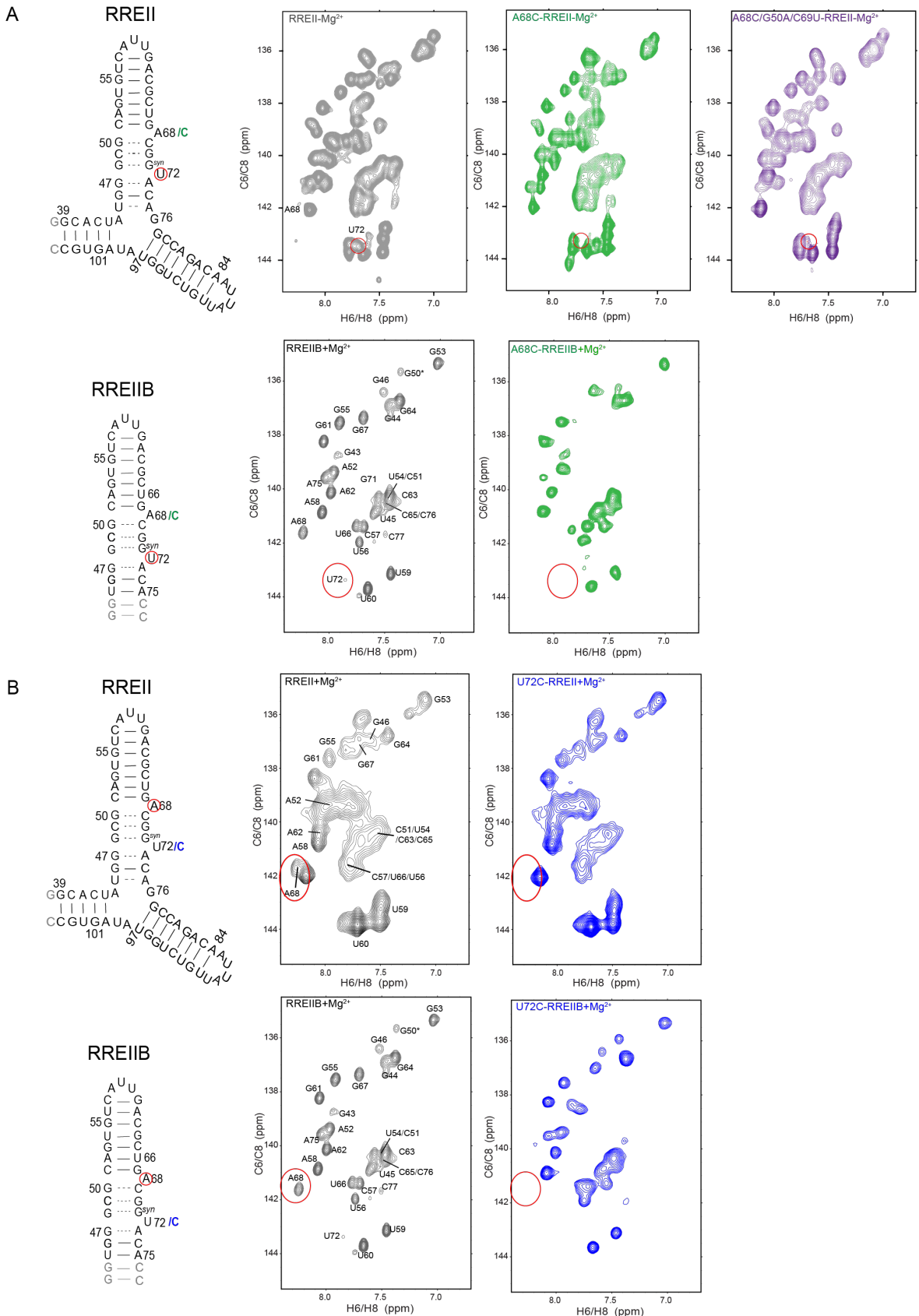


**Figure S7.** NMR spectra and assignments for ES2 stabilizing mutant (UUCG-G48A/G50U) at 25 °C. Secondary structure of UUCG-G48A/G50U based on NMR data. Base pairs with and without detectable H-bonds are indicated using solid and dashed lines, respectively. The imino resonances for the base pairs around the C69 and G70 bulge were not observed likely due to increase solvent exchange and possibly also conformational exchange. The G47-H1 imino resonance G47H8-H1' NOEs consistent with a G47(*anti*)-A73(*anti*) base pair were observed at pH 6.4 while the imino resonance was broadened significantly at pH 5.4, consistent with the behavior seen with the UUCG-RRE20 mutant. For other non-exchangeable proton, the NOE connectivity breaks at A68-C69 and G70-G71 consistent with C69 and G70 adopting a bulge conformation, whereas uninterrupted intra- and inter-nucleotide H8/6-H1' NOEs were observed for all other nucleotides consistent with the proposed secondary structure. The sample condition was 1.8 mM UUCG-G48A/G50U in 15 mM sodium phosphate, 25 mM NaCl, 0.1 mM EDTA, with or without 3 mM MgCl<sub>2</sub>.



**Figure S8.** NMR spectra and assignments for ES knockout mutant m<sup>3</sup>U72-RREIIB measured at 25 °C. (A) The secondary structure of RREIIB and m<sup>3</sup>U72-RREIIB based on NMR data. Residues showing significant RDs ( $p_B > 15\%$ ,  $\Delta\omega > 1.5$  ppm) or larger differences in chemical shifts between m<sup>3</sup>U72-RREIIB and RREIIB are highlighted using red circles on RREIIB and green circles on m<sup>3</sup>U72-RREIIB respectively. Resonances with significant RD (outside from the modified residue) are expected to show larger

perturbations toward GS due to suppression of ESs in  $m^3\text{U72-RREIIB}$ . Indeed, G71-C8H8 and G47-C8H8 which have large RD, show large changes ( $\sim 0.3$  ppm) toward the GS chemical shift measured by RD in the absence of  $\text{Mg}^{2+}$  (red dashed lines). U72 resonance experiences perturbations due to the modification. Chemical shift perturbations at G48-C8H8 and G50-C8H8 (+ $\text{Mg}^{2+}$ ) which have no RDs could result from slight changes in the GS with introduction of the modification. (B) Normalized resonance intensities measured for RREIIB and  $m^3\text{U72-RREIIB}$  in the presence of 3 mM  $\text{Mg}^{2+}$ . A52-C8H8, A52-C2H2 and U56-C6H6 were used as a reference and normalized to 0.1. G48, G71 and A73, which experience line-broadening due to exchange with ES, show increased intensities in  $m^3\text{U72-RREIIB}$  consistent with suppression of the exchange. The sample condition was 1.5 mM  $m^3\text{U72-RREIIB}$  in 15 mM sodium phosphate, 25 mM NaCl, 0.1 mM EDTA, with or without 3 mM  $\text{MgCl}_2$ .



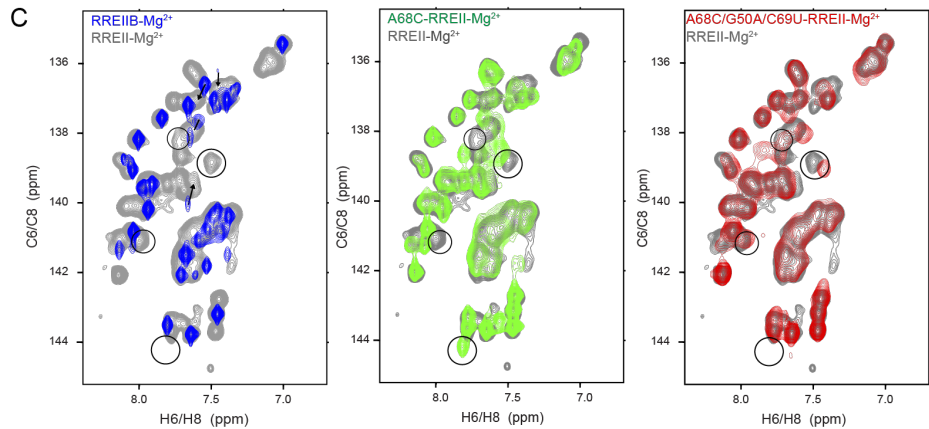


**Figure S9.** NMR spectra of RREII and RREIIB mutants used in fluorescence binding studies measured at 25 °C. (A, B) Residues that experience broadening due to micro-to-millisecond exchange are highlighted using red circles on the secondary structure. (A) In both ES2-stabilizing A68C-RREII and A68C-RREIIB, U72-C6 was significantly broadened (highlighted in a circle), consistent with a bias toward ES2, and this broadening was partially rescued in the A68C/G50A/C69U-RREII rescue mutant. (B) In both ES-stabilizing U72C-RREII and U72C-RREIIB, A68-C8 was significantly broadened (highlighted in a circle) consistent with a bias toward the ES1 and ES2. (C) Spectra showing that the ES-stabilizing mutation A68C induces long-range perturbations (highlighted in circles) at nucleotides remote from the stem IIB. In order to compare potentially dynamic residues, NMR spectra in the absence of Mg<sup>2+</sup> were compared to avoid further line broadening. The sample conditions were 0.5-0.6 mM RREII or RREIIB in 15 mM sodium phosphate, 25 mM NaCl, 0.1 mM EDTA, pH 6.4 with or without 3 mM MgCl<sub>2</sub>.

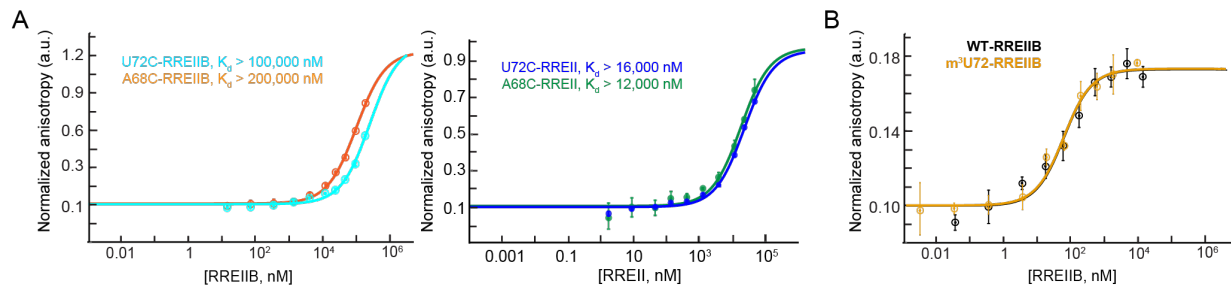


**Figure S10.** Measurement of the binding affinity between Rev-ARM peptide and ES-stabilizing mutants, and ES knockout mutant using fluorescence polarization. (A) Normalized anisotropy values measured for ES stabilizing mutants with higher RRE mutant concentrations using with one-site binding model (see methods). Due to the lower binding affinity, the binding curves did not reach saturation, and further addition of ES-stabilizing mutants resulted in additional low-affinity binding. (B) Normalized anisotropy values measured for RREIIB and  $m^3U72\text{-}RREIIB$  ES knockout mutant fitted with one-site binding model (see methods). The anisotropy value observed in the absence of RNA was normalized to 0.1. Uncertainty reflects the standard deviation from three independent measurements. Buffer conditions: 30 mM HEPES, pH= 7.0, 100 mM KCl, 10mM sodium phosphate, 10 mM ammonium acetate, 10 mM guanidinium chloride, 2 mM MgCl<sub>2</sub>, 20 mM NaCl, 0.5 mM EDTA, and 0.001% (v/v) Triton-X100. Concentration of Rev-Fl peptide was 10 nM and 1 nM for RREIIB and RREII respectively.

**Table S1.** Exchange parameters obtained from fitting  $R_{1p}$  data measured on RREIIB.

<i>Nuclei</i>	$\Delta\omega_{ES1}$ (ppm)	$pop_{ES1}$ (%)	$k_{ex\_ES1}$ (s <sup>-1</sup> )	$\Delta\omega_{ES2}$ (ppm)	$pop_{ES2}$ (%)	$k_{ex\_ES2}$ (s <sup>-1</sup> )	$R_1$ (s <sup>-1</sup> )	$R_2$ (s <sup>-1</sup> )	<i>Red. <math>\chi^2</math></i>
<b>+Mg<sup>2+</sup></b>									
U72-C8	-2.3± 0.1						0.0± 0.6	60.4± 3.6	
G46-C8	1.1± 0.1	17.5 ± 2.1	6195 ± 423	1.1± 0.1			0.8± 0.3	67.6± 1.3	
G67-C8				0.9± 0.02	3.9 ± 0.1	2364 ± 53	1.0 ± 0.1	65.7± 0.3	0.28
A68-C8				-2.5± 0.03			0.8 ± 0.2	45.2± 0.4	
<b>-Mg<sup>2+</sup></b>									
U72-C8	-2.6± 0.1			-0.5± 0.04			0.7± 0.1	48.5± 1.1	
G71-C8	-3.8± 0.2			-1.6± 0.05			0.2± 0.7	99.0± 3.7	
G47-C8	4.0± 0.2	5.7± 0.4	10751± 442	1.6± 0.05			1.0± 0.5	51.7± 2.9	
G46-C8	1.3± 0.1			0.7± 0.02	11.0± 0.4	2311± 109	0.5± 0.1	48.8± 1.0	0.45
G67-C8				0.4± 0.02			0.7± 0.2	54.6± 0.5	
A68-C8				-2.4± 0.07			0.0± 1.2	53.7± 2.6	

**Table S2:** List of spin-lock powers and offsets used in the  $R_{1p}$  experiments at 25 °C. Shown are on-resonance spin-lock power ( $\omega 2\pi^{-1}$ ) or off-resonance spin-lock ( $\omega 2\pi^{-1}$ ) at variable offsets ( $\Omega 2\pi^{-1}$ ) indicated as “ $\omega 2\pi^{-1}$  &  $\pm [\Omega 2\pi^{-1}]$ ”

RREIIB with 3mM Mg <sup>2+</sup>	On-resonance spinlock power (Hz)/Off-resonance spinlock power (Hz) with [offsets]
U72-C6	100, 150, 200, 250, 300, 400, 500, 700, 1000, 1200, 1600, 2000, 2400, 2800
	200 & [-600] $\pm$ [50, 100, 150, 200, 250, 300, 400, 500]
	400 & [900, -800] $\pm$ [50, 100, 200, 300, 400, 500, 600, 700, 800, 1000, 1100, 1300]
	700 & $\pm$ [100, 200, 300, 400, 500, 700, 900, 1100, 1300, 1500, 1700]
	1000 & $\pm$ [100, 200, 300, 400, 500, 700, 900, 1100, 1300, 1500, 1700, 1900, 2200]
G46-C8	100, 150, 200, 250, 300, 400, 500, 700, 900, 1200, 1600, 2000, 2400, 2800
	150 & $\pm$ [50, 100, 150, 200, 250, 300, 350, 400, 450]
	300 & $\pm$ [50, 100, 150, 200, 250, 300, 400, 500, 600, 750, 900]
	500 & $\pm$ [100, 200, 300, 400, 500, 600, 700, 800, 900, 1100, 1300]
	700 & $\pm$ [100, 200, 300, 400, 500, 600, 700, 800, 900, 1100, 1300, 1500, 1700]
A68-C8	100, 150, 200, 250, 300, 400, 500, 700, 900, 1200, 1600, 2000, 2400, 2800
	200 & [-600] $\pm$ [50, 100, 150, 200, 250, 300, 400, 500]
	400 & [900, -800] $\pm$ [50, 100, 200, 300, 400, 500, 600, 700, 800, 1000, 1100, 1300]
	700 & $\pm$ [100, 200, 300, 400, 500, 700, 900, 1100, 1300, 1500, 1700]
	1000 & $\pm$ [100, 200, 300, 400, 500, 700, 900, 1100, 1300, 1500, 1700, 1900, 2200]
G67-C8	100, 150, 200, 250, 300, 400, 500, 700, 900, 1200, 1600, 2000, 2400, 2800
	150 & $\pm$ [50, 100, 150, 200, 250, 300, 350, 400, 450]
	300 & $\pm$ [50, 100, 150, 200, 250, 300, 400, 500, 600, 750, 900]
	500 & $\pm$ [100, 200, 300, 400, 500, 600, 700, 800, 900, 1100, 1300]
	700 & $\pm$ [100, 200, 300, 400, 500, 600, 700, 800, 900, 1100, 1300, 1500, 1700]
A75-C8	250, 400, 500, 700, 900, 1200, 1600, 2000, 2400, 2800
	400 & $\pm$ [100, 200, 300, 400, 500, 600, 700, 900, 1100]
	700 & $\pm$ [100, 200, 300, 400, 500, 600, 700, 800, 900, 1100, 1300, 1500, 1700]
	1000 & $\pm$ [100, 200, 300, 400, 500, 600, 700, 800, 900, 1100, 1300, 1500, 1700, 2000, 2300, 2600]
A52-C8	150, 200, 250, 300, 400, 500, 700, 900, 1200, 1600, 2000, 2400, 2800
	200 & $\pm$ [50, 100, 150, 200, 250, 300, 400, 500, 600]
	400 & $\pm$ [100, 200, 300, 400, 500, 600, 700, 900, 1100]
	700 & $\pm$ [100, 200, 300, 400, 500, 600, 700, 800, 900, 1100, 1300, 1500, 1700]
	1000 & $\pm$ [100, 200, 300, 400, 500, 600, 700, 800, 900, 1100, 1300, 1500, 1700, 2000, 2300, 2600]
U66-C6	150, 200, 250, 300, 400, 500, 700, 1000, 1200, 1600, 2000, 2400, 2800
	250 & $\pm$ [50, 100, 150, 200, 250, 300, 400, 500, 600]
	400 & $\pm$ [100, 200, 300, 400, 500, 600, 700, 900, 1100, 1300]

	700 & $\pm$ [100, 200, 300, 400, 500, 700, 900, 1100, 1300, 1500, 1700]
	1000 & $\pm$ [100, 200, 300, 400, 500, 700, 900, 1100, 1300, 1500, 1700, 1900, 2200]
G53-C8	150, 200, 250, 300, 400, 500, 700, 900, 1200, 1600, 2000, 2400, 2800
	200 & $\pm$ [50, 100, 150, 200, 250, 300, 400, 500, 600]
	400 & $\pm$ [100, 200, 300, 400, 500, 600, 700, 900, 1100]
	700 & $\pm$ [100, 200, 300, 400, 500, 600, 700, 800, 900, 1100, 1300, 1500, 1700]
	1000 & $\pm$ [100, 200, 300, 400, 500, 600, 700, 800, 900, 1100, 1300, 1500, 1700, 2000, 2300, 2600]

RREIIB without Mg <sup>2+</sup>	On-resonance spinlock power (Hz)/Off-resonance spinlock power (Hz) with [offsets]
U72-C6	100, 150, 200, 250, 300, 400, 500, 700, 900, 1200, 1600, 2000, 2400, 2800
	200 & $\pm$ [50, 100, 150, 200, 250, 300, 400, 500, 600]
	500 & $\pm$ [100, 200, 300, 400, 500, 600, 700, 900, 1100, 1400]
	800 & $\pm$ [100, 200, 300, 400, 500, 600, 700, 900, 1100, 1300, 1600, 1900, 2200]
	1200 & $\pm$ [100, 200, 300, 400, 500, 600, 800, 1100, 1400, 1800, 2200, 2700, 3200]
	1600 & $\pm$ [100, 200, 300, 500, 700, 900, 1200, 1600, 2000, 2400, 2800, 3200, 3600, 4000]
G71-C8	150, 200, 250, 300, 400, 500, 700, 900, 1200, 1600, 2000, 2400, 2800
	200 & $\pm$ [50, 100, 150, 200, 250, 300, 400, 500, 600]
	400 & $\pm$ [100, 200, 300, 400, 500, 600, 700, 900, 1100]
	700 & $\pm$ [100, 200, 300, 400, 500, 600, 700, 800, 900, 1100, 1300, 1500, 1700]
	1000 & $\pm$ [100, 200, 300, 400, 500, 600, 700, 800, 900, 1100, 1300, 1500, 1700, 2000, 2300, 2600]
G47-C8	150, 200, 250, 300, 400, 500, 700, 900, 1200, 1600, 2000, 2400, 2800
	400 & $\pm$ [100, 200, 300, 400, 500, 600, 700, 900, 1100]
	700 & $\pm$ [100, 200, 300, 400, 500, 600, 700, 800, 900, 1100, 1300, 1500, 1700]
	1000 & $\pm$ [100, 200, 300, 400, 500, 600, 700, 800, 900, 1100, 1300, 1500, 1700, 2000, 2300, 2600]
G46-C8	100, 150, 200, 250, 300, 400, 500, 700, 900, 1200, 1600, 2000, 2400, 2800
	150 & $\pm$ [50, 100, 150, 200, 250, 300, 350, 400]
	200 & $\pm$ [50, 100, 150, 200, 250, 300, 400, 500, 600]
	300 & $\pm$ [100, 200, 300, 400, 500, 600, 700, 900]
	400 & $\pm$ [100, 200, 300, 400, 500, 600, 700, 900, 1100]
	700 & $\pm$ [100, 200, 300, 400, 500, 600, 700, 800, 900, 1100, 1300, 1500, 1700]
A68-C8	100, 150, 200, 250, 300, 400, 500, 700, 900, 1200, 1600, 2000, 2400, 2800
	150 & $\pm$ [50, 100, 150, 200, 250, 300, 350, 400]
	200 & $\pm$ [50, 100, 150, 200, 250, 300, 400, 500, 600]
	300 & $\pm$ [100, 200, 300, 400, 500, 600, 700, 800, 900]
	400 & $\pm$ [100, 200, 300, 400, 500, 600, 700, 900, 1100]
	700 & $\pm$ [100, 200, 300, 400, 500, 600, 700, 800, 900, 1100, 1300, 1500, 1700]
G67-C8	100, 150, 200, 250, 300, 500, 700, 900, 1200, 1600, 2000, 2400, 2800

	200 & $\pm$ [50, 100, 150, 200, 250, 300, 400, 500, 600]
	300 & $\pm$ [100, 200, 300, 400, 500, 600, 700, 800, 900]
	400 & $\pm$ [100, 200, 300, 400, 500, 600, 700, 900, 1100]
	700 & $\pm$ [100, 200, 300, 400, 500, 600, 700, 800, 900, 1100, 1300, 1500, 1700]
A75-C8	150, 200, 250, 300, 400, 500, 700, 900, 1200, 1600, 2000, 2400, 2800
	200 & $\pm$ [50, 100, 150, 200, 250, 300, 400, 500, 600]
	400 & $\pm$ [100, 200, 300, 400, 500, 600, 700, 900, 1100]
	700 & $\pm$ [100, 200, 300, 400, 500, 600, 700, 800, 900, 1100, 1300, 1500, 1700]
	1000 & $\pm$ [100, 200, 300, 400, 500, 600, 700, 800, 900, 1100, 1300, 1500, 1700, 2000, 2300, 2600]
A52-C8	150, 200, 250, 300, 400, 500, 700, 900, 1200, 1600, 2000, 2400, 2800
	200 & $\pm$ [50, 100, 150, 200, 250, 300, 400, 500, 600]
	400 & $\pm$ [100, 200, 300, 400, 500, 600, 700, 900, 1100]
	700 & $\pm$ [100, 200, 300, 400, 500, 600, 700, 800, 900, 1100, 1300, 1500, 1700]
	1000 & $\pm$ [100, 200, 300, 400, 500, 600, 700, 800, 900, 1100, 1300, 1500, 1700, 2000, 2300, 2600]

RREIIB at pH 8	On-resonance spinlock power (Hz)/Off-resonance spinlock power (Hz) with [offsets]
G47-C8	100, 150, 200, 250, 300, 400, 500, 700, 900, 1200, 1600, 2000, 2400, 2800
	200 & $\pm$ [50, 100, 150, 200, 250, 300, 400, 500, 600]
	600 & $[\pm 100, \pm 200, \pm 300, \pm 400, \pm 500, \pm 600, \pm 700, \pm 900, \pm 1100, \pm 1400, \pm 1700]$
	1000 & $[\pm 100, \pm 200, \pm 300, \pm 400, \pm 500, \pm 600, \pm 800, \pm 1100, \pm 1400, \pm 1800, \pm 2200, \pm 2700, \pm 3200]$
	1600 & $[\pm 100, \pm 200, \pm 300, \pm 500, \pm 700, \pm 900, \pm 1200, \pm 1600, \pm 2000, \pm 2400, \pm 2800, \pm 3200, \pm 3600, \pm 4000]$
A68-C8	100, 150, 200, 250, 300, 400, 500, 700, 900, 1200, 1600, 2000, 2400, 2800
	200 & $\pm$ [50, 100, 150, 200, 250, 300, 400, 500, 600]
	600 & $[\pm 100, \pm 200, \pm 300, \pm 400, \pm 500, \pm 600, \pm 700, \pm 900, \pm 1100, \pm 1400, \pm 1700]$
	1000 & $[\pm 100, \pm 200, \pm 300, \pm 400, \pm 500, \pm 600, \pm 800, \pm 1100, \pm 1400, \pm 1800, \pm 2200, \pm 2700, \pm 3200]$
	1600 & $[\pm 100, \pm 200, \pm 300, \pm 500, \pm 700, \pm 900, \pm 1200, \pm 1600, \pm 2000, \pm 2400, \pm 2800, \pm 3200, \pm 3600, \pm 4000]$

## REFERENCE

1. Parisien, M. and Major, F. (2008) The MC-Fold and MC-Sym pipeline infers RNA structure from sequence data. *Nature*, **452**, 51-55.